

Article

A Nanodiamond-Based Electrochemical Sensor for the Determination of Paracetamol in Pharmaceutical Samples

Déborah de Oliveira Lopes ¹, Felipe Magalhães Marinho ¹, Patricia Batista Deroco ², Amanda Neumann ³, Jessica Rocha Camargo ³, Rafaela Cristina de Freitas ³, Lucas Ventosa Bertolim ³, Orlando Fatibello Filho ⁴, Bruno Campos Janegitz ^{3,*} and Geiser Gabriel de Oliveira ¹

¹ Collegiate Chemistry, Federal University of Tocantins, Gurupi 77402-970, TO, Brazil; oliveira.lopes@mail.uft.edu.br (D.d.O.L.); magalhaes.marinho@mail.uft.edu.br (F.M.M.); geiser@mail.uft.edu.br (G.G.d.O.)

² Institute of Chemistry, University of Campinas, Campinas 13083-970, SP, Brazil; pderoco@unicamp.br

³ Department of Nature Sciences, Federal University of São Carlos, Mathematics and Education, Araras 13600-970, SP, Brazil; amandaneumann@estudante.ufscar.br (A.N.); jessicacamargo@estudante.ufscar.br (J.R.C.); rafaelafreitas@estudante.ufscar.br (R.C.d.F.); l.vbertolim@estudante.ufscar.br (L.V.B.)

⁴ Department of Chemistry, Federal University of São Carlos, São Carlos 13565-905, SP, Brazil; bello@ufscar.br

* Correspondence: brunocj@ufscar.br

Abstract: This study presents an electrochemical sensor developed from a glassy carbon electrode modified with nanodiamond film (ND/GCE). This electrochemical response of the proposed sensor was improved, and it showed excellent analytical performance for the detection of paracetamol (PAR), which was attributed to the high PAR charging capacity on the electrode surface and the excellent electrical conductivity of ND. Morphological and electrochemical characterizations of the sensor were performed via scanning electron microscopy (SEM) and cyclic voltammetry using a redox probe $[\text{Fe}(\text{CN})_6]^{3-}$. The sensor was applied for the determination of PAR. Quantification was performed using square-wave voltammetry, and it showed a linear concentration range from 0.79 to 100 $\mu\text{mol L}^{-1}$, with a limit of detection of 0.18 $\mu\text{mol L}^{-1}$. The proposed sensor exhibited satisfactory repeatability and high sensitivity in the determination of the analyte of interest. The electrochemical sensor was also employed for the analysis of PAR in real samples, with recovery rates ranging between 96.4 and 98.7%. This sensor was successfully used for the determination of the drug in pharmaceutical samples.

Keywords: nanodiamond; paracetamol; acetaminophen; square-wave voltammetry; electrochemical sensors



Citation: de Oliveira Lopes, D.; Magalhães Marinho, F.; Batista Deroco, P.; Neumann, A.; Rocha Camargo, J.; Cristina de Freitas, R.; Ventosa Bertolim, L.; Fatibello Filho, O.; Campos Janegitz, B.; Oliveira, G.G.d. A Nanodiamond-Based Electrochemical Sensor for the Determination of Paracetamol in Pharmaceutical Samples.

Chemosensors **2024**, *12*, 243.

<https://doi.org/10.3390/chemosensors12110243>

Received: 7 October 2024

Revised: 11 November 2024

Accepted: 15 November 2024

Published: 20 November 2024



Copyright: © 2024 by the authors. Licensee MDPI, Basel, Switzerland. This article is an open access article distributed under the terms and conditions of the Creative Commons Attribution (CC BY) license (<https://creativecommons.org/licenses/by/4.0/>).

1. Introduction

Nanodiamonds (NDs) have attracted considerable attention in recent years due to their exceptional properties, which make them an ideal material for the development of electrochemical sensors [1,2]. These nanospheres, which are primarily composed of sp^3 carbons and some sp^2 carbons, exhibit excellent hardness, a wide potential window, and a low background current in both aqueous and non-aqueous solutions. Their high chemical and electrochemical stability, biocompatibility, low toxicity, and excellent corrosion resistance further enhance their applicability in various fields [3]. Originally synthesized from explosive detonations in the 1960s, NDs have been used as a material since the 1990s [3,4]. The versatility of NDs allows for the surface modification of working electrodes, which facilitates the electrochemical detection of drugs such as paracetamol (PAR). Their applications extend beyond sensing and include areas such as drug delivery [5], bioimaging [6], energy storage [7] catalysis [8], and photodevices [9]. In particular, NDs have shown significant potential in electrochemical sensors [10–14]. This material can be

synthesized through detonation techniques, high pressure and high temperatures, high-pressure and high-temperature (HPHT) ball milling, laser ablation, and chemical vapor deposition (CVD) [15]. The main applications of this material are as fluorescent particles to obtain biomedical images [1], tribology and lubrication [16], drug delivery, bioimaging biosensors [17], and energy storage catalysis. Acetaminophen (N-acetyl-p-aminophenol), commonly known as PAR, is a widely used antipyretic and analgesic drug effective for headache, migraine, and arthritis [18,19]. However, the risk of overdose or chronic use can lead to kidney and liver damage due to the accumulation of toxic metabolites [20–22]. Additionally, its hydrolytic degradation product, 4-aminophenol, has teratogenic effects and is nephrotoxic [23,24]. Therefore, the development of sensitive and accurate analytical methods for the determination of PAR concentrations in pharmaceutical preparations and human plasma is decisive in effective health management [23].

Various analytical techniques have been used to quantify PAR, including colorimetry [25], titrimetry [26], FTIR and Raman spectrometry [27–31], and liquid chromatography [31,32]. Despite their effectiveness, these methods often present limitations, such as high costs, long analysis times, and the need for sample pretreatment, making them unsuitable for routine analysis [33,34]. In contrast, electrochemical techniques have proven to be a promising alternative due to their high sensitivity and lower costs.

This study introduces a newly developed electrochemical sensor fabricated with ND-modified glassy carbon electrodes (GCEs). The electrochemical properties of this sensor were investigated, and its potential for the sensitive determination of PAR in pharmaceutical products using the square-wave voltammetry (SWV) technique was demonstrated. The integration of NDs into sensor design highlights the growing interest in the use of advanced materials for improved analytical applications.

2. Materials and Methods

2.1. Reagents and Solutions

ND powder (<10 nm particle size) and PAR were purchased from Sigma-Aldrich® (St. Louis, MO, USA). All other chemical reagents were of analytical grade and used as received from the respective suppliers. The aqueous solutions were prepared using deionized water, and the suspension was prepared using ultrapure water (resistivity > 18.0 MΩ cm) supplied via a Milli-Q (Millipore -Merck group, Burlington, MA, USA) purification system. Sodium hydroxide (NaOH), sulfuric acid (H₂SO₄), potassium chloride (KCl), and potassium ferricyanide (K₃[Fe(CN)₆]) were purchased from all Synth® (Zola Predosa, Italy). The 0.1 mol L⁻¹ of NaOH solution was used to adjust and maintain the desired pH ranges. The PAR stock solutions used were prepared daily before each study from an H₂SO₄ solution (0.1 mol L⁻¹) to obtain a concentration of 0.1 mol L⁻¹. Subsequent concentrations were prepared via dilution.

2.2. Apparatus

ND voltametric measurements were performed using a Potentiostat/Galvanostat—PG580 (Uniscan Instruments, Buxton, UK) interfaced with a computer managed using the UiChem software version 6.62 for the acquisition of voltametric data. Voltammograms were obtained from a glass electrochemical cell with holes for coupling electrodes: the working electrode was an ND/GCE, platinum counter-electrode, and the Ag/AgCl reference electrode was KCl, 3.0 mol L⁻¹.

A morphologic analysis of the nanomaterials was carried out via scanning electron microscopy (SEM) using a Thermo Scientific Prisma E Scanning Electron Microscope (Waltham, MA, USA) with ColorSEM Technology and integrated into energy-dispersive X-ray spectroscopy (EDS) (São Paulo, Brazil), operating at 20 kV. The X-ray diffraction (XRD) was carried out using a Miniflex II X-ray diffractometer (Rigaku, Tokyo, Japan), from a 10° to a 90° angular recording range.

2.3. Preparation of Working Electrode

Before the modification, the surface of the electrode was carefully polished using extra fine carborundum paper. Then, the electrode was then sonicated in isopropyl alcohol for 1 min, washed with water, and dried. Then, 1.0 mg ND was suspended in 1.0 mL of ultrapure water. The suspension was dispersed using ultrasonic stirring for 30 min. In the end, 8.0 μL of the dispersion was deposited on the surface of the electrode using the drop-casting method and dried at room temperature for approximately 2 h until the complete drying and formation of the thin film; see Figure 1.

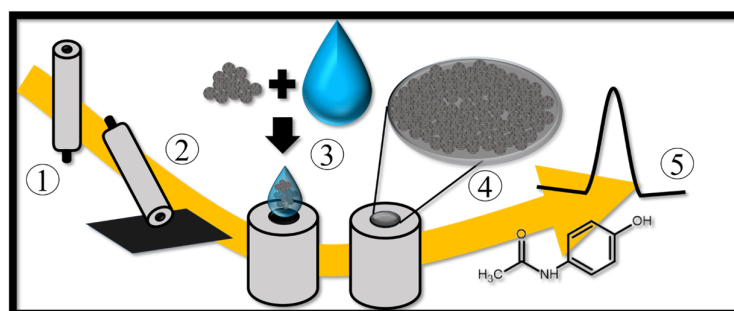


Figure 1. Scheme of ND/GCE preparation. The bare electrode was cleaned (step 1); the surface of the electrode was polished carefully using extra fine carborundum paper (step 2), and the polished electrode was sonicated in isopropyl alcohol for 1 min and then rinsed with water and then dried. Then, 1.0 mg of ND was suspended in 1.0 mL of ultrapure water, and the suspension was ultrasonically stirred for 30 min to achieve proper dispersion (step 3); 8.0 μL of the ND dispersion was deposited on the electrode surface using the drop-casting method, followed by drying at room temperature for 2 h to form the film (step 4). Finally, the ND/GCE was ready to use in PAR detection (Step 5).

2.4. Preparation of Samples

A total of 10 tablets of PAR (paracetamol, 500 mg and 750 mg) formulations were accurately weighed and finely ground in a mortar. A chosen amount of this powder was transferred into a 200 mL volumetric flask. About 50 mL of NaOH (0.1 mol L^{-1}) was added, swirled, and sonicated for 15 min. The volume of the sample was completed to the mark and finally filtered using fine filter paper. The first portion of the filtrate was rejected. A specific volume of the stock solution of the drugs was diluted with deionized water to obtain the suitable concentration.

As a comparative method, the spectrophotometric procedure described in the Brazilian Pharmacopoeia [35] was used for the determination of paracetamol in commercial samples, which were performed in a spectrophotometer, Spectrovision-T60 (Techcomp Ltd., Hong Kong, China), using quartz cells with a 1.00 cm optical path and $\lambda = 190\text{--}1100 \text{ nm}$.

3. Results and Discussion

3.1. Morphological and Structural Characterizations

Morphological characterizations of NDs utilized for the GCE modification were studied by SEM analysis with and without the elemental analysis using ColorSEM technology. These images are presented in Figure 2, with SEM magnifications of $2000\times$ and $4000\times$, in Figure 2A and B, respectively. In these images, it is possible to observe the success of the dispersion of NDs due to its homogeneity, presenting particles as spherical clusters on all the surfaces analyzed, with an average of 900 nm diameter per cluster. Figure 2C presents the ColorSEM image, in $2000\times$ magnification, showing the presence of carbon, which can also be observed in Figure 2D by the peaks in the EDS. Otherwise, the oxygen quantities calculated in this analysis are negligible compared to the carbon quantities.

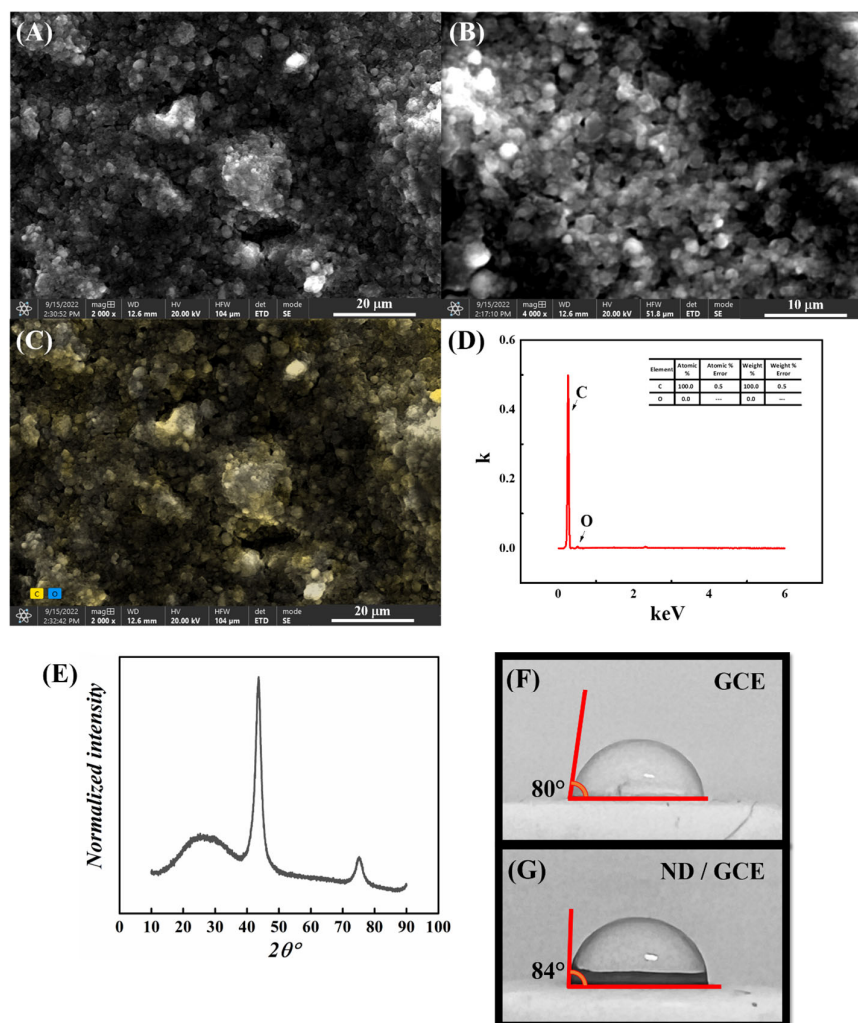


Figure 2. SEM images obtained via ND surfaces with magnifications of (A) 2000 \times and (B) 4000 \times ; (C) ColorSEM image of ND surfaces with a magnification of 2000 \times ; (D) X-ray diffraction pattern of NDs, $2\theta = 10$ to 90° ; (E) energy-dispersive X-ray spectroscopy (EDS) mapping for NDs and contact angle wettability for (F) GCE and (G) ND/GCE.

XRD analysis was performed to confirm the structure of this dispersion, and the X-ray diffraction pattern is present in Figure 2E. It is possible to observe two expressive peaks at $2\theta = 44.0^\circ$ and 75.6° , which correspond to 111 and 220 crystalline plans for NDs, respectively, as presented in the literature [36,37]. To measure the contact angles, an 8 μ L aliquot of ultrapure water was dropped onto the surface of a GCE, and the sensor was modified with the proposed ND film. Photos were taken 30 s after the droplet was applied. Depending on the observed contact angle (θ) with the water, the surface can be classified as super hydrophilic ($\theta < 10^\circ$), hydrophilic ($\theta < 90^\circ$), hydrophobic ($90^\circ < \theta < 150^\circ$), or superhydrophobic ($\theta > 150^\circ$) [38]. Thus, the unmodified and modified sensor surfaces displayed hydrophilic profiles, with contact angles of $80 \pm 1^\circ$ for GCE and $84 \pm 1^\circ$ for ND/GCE (Figure 2F,G).

3.2. Electrochemical Characterizations

The electrochemical profile of the bare GCE and ND/GCE were investigated using the cyclic voltammetry technique with a redox probe $[\text{Fe}(\text{CN})_6]^{3-}$ in 0.1 mol L^{-1} of KCl. Cyclic voltammograms comparing GCE and ND/GCE in the presence of 9.9×10^{-4} mol L^{-1} $[\text{Fe}(\text{CN})_6]^{3-}$ in 0.1 mol L^{-1} of KCl at a scan rate of $v = 50$ mV s^{-1} are shown in Figure 3A. At a scan rate of 50 mV s^{-1} , ND/GCE presented a ratio of the anodic and cathodic peak

current (I_{p_a}/I_{p_c}) of 0.93 and a peak potential separation (ΔE_p) of 110 mV, and the bare GCE presented an I_{p_a}/I_{p_c} of 0.88 and a ΔE_p of 238 mV; see Figure 3B.

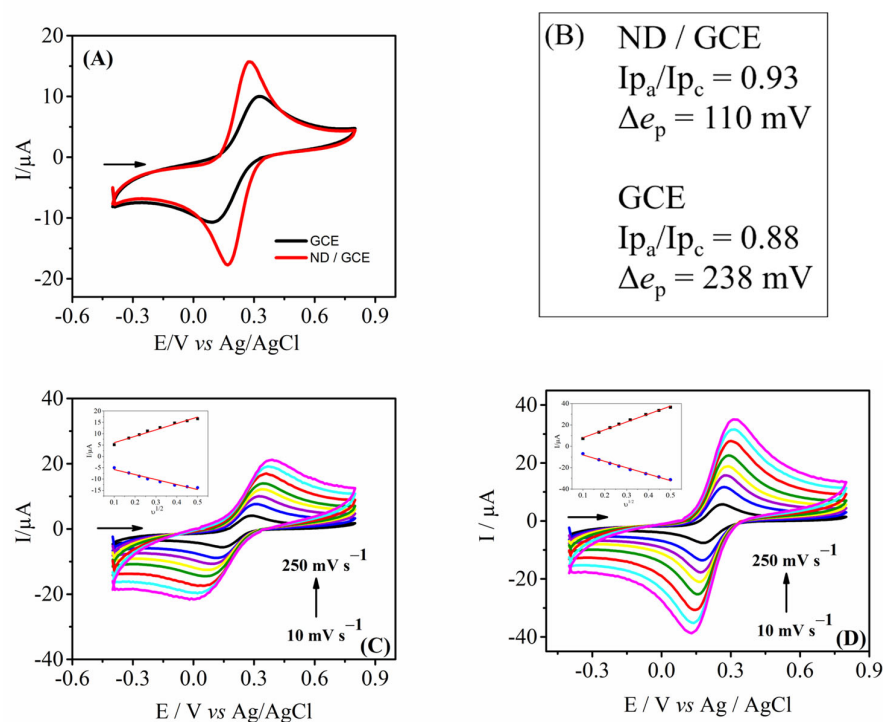


Figure 3. Cyclic voltammograms comparing GCE and ND/GCE in the presence of 9.9×10^{-4} mol L^{-1} $[Fe(CN)_6]^{3-}$ in 0.1 mol L^{-1} of KCl at a scan rate of 50 mV s^{-1} are shown in (A); (B) presents the I_{p_a}/I_{p_c} ratio and ΔE_p values for both GCE and ND/GCE electrodes; (C,D) cyclic voltammograms obtained for GCE and ND/GCE electrodes, respectively, in the presence of 9.9×10^{-4} mol L^{-1} $[Fe(CN)_6]^{3-}$ in 0.1 mol L^{-1} of KCl at scan rates ranging from 50 to 200 mV s^{-1} . Insets: correlation I vs. $v^{1/2}$.

The scan-rate study was carried out with a range of 10 to 250 mV s^{-1} ($10, 30, 50, 70, 100, 150, 200,$ and 250 mV s^{-1}), present in Figure 2C for GCE and Figure 2D for ND/GCE. ND/GCE presented a better peak definition compared to the bare GCE in both processes. In this context, ND/GCE also presented reversibility closer to the theoretical values for quasi-reversible systems. Through these analyses, an I vs. $v^{1/2}$ correlation was plotted, which is inserted into Figure 3C,D for the respective data, where both systems presented a linearity close to 1, with an R^2 equal to 0.979 and 0.995, respectively, which confirms the majority of a diffusional controlled process.

Considering this linearity, the electroactive area of each electrode was calculated using the Randles–Sevcik equation, Equation (1) [39]:

$$I_p = \pm(2.69 \times 10^5)n^{3/2}AD^{1/2}v^{1/2}C, \quad (1)$$

where I_p is the peak current, n is the number of electrons transferred ($n = 1$), A is the electroactive surface area, D is the diffusion coefficient ($D = 6.2 \times 10^{-6} \text{ cm}^2 \text{ s}^{-1}$) for $[Fe(CN)_6]^{3-}$, v is the scan rate, and C is the redox probe concentration in bulk solution ($9.9 \times 10^{-7} \text{ mol cm}^{-3}$). Therefore, the electroactive area increased from 0.038 cm^2 to 0.100 cm^2 by a factor of $2.6 \times$ after the ND modification, presented in Table S1. Additionally, the electroactive area of the ND/GCE also presented an increase above the geometric area of 0.071 cm^2 .

According to the relation of " ψ "— ΔE_p [40], the charge-transfer reaction rate constant (k^0) can be estimated for GCE and ND/GCE using the Nicholson equation; see Equation (2) [41],

$$\psi = k^0 \left(\frac{\pi D n \nu F}{RT} \right)^{-1/2} \quad (2)$$

where k^0 is the heterogeneous electron transfer rate constant (cm s^{-1}), " ψ " is a kinetic parameter dependent on the scan rate that can be calculated from the equation proposed by Lavagnini et al. [42], F is the Faraday's constant ($96,485 \text{ C mol}^{-1}$), $R = 8.314 \text{ J mol}^{-1} \text{ K}^{-1}$, $T = 298.15 \text{ K}$, and other parameters are as utilized for the electroactive area calculus.

With the ψ values known, k^0 is directly determined as being the slope of the ψ versus a $36.33 \text{ v}^{-1/2}$ curve. The 36.33 factor is equivalent to the term $[\pi D n F / (RT)]^{-1/2}$ of the Nicholson equation (Equation (2)). The obtained k^0 values are also presented in Table S1, and as can be seen, the electron transfer rate constant was enhanced approximately 4 times. Through the data presented in Table S1, it was observed that the modification of the electrode with ND favored its electrical conductivity, that is, its ability to exchange electrons. Therefore, ND was able to improve the electrochemical features of the bare GCE, proving its potential for application in the design of modified electrochemical sensors.

3.3. Electrochemical Detection of Paracetamol

An electrochemical analysis using cyclic voltammetry was performed to evaluate the response profile of the PAR compound on the bare GCE and ND/GCE; the results are displayed in Figure 4A. Well-defined anodic peaks are observed in both curves, while no reduction peaks are evident. For the bare GCE, the oxidation peak potential was 804 mV with an anodic peak current of 11.6 μA ; by contrast, the ND/GCE was 750 mV, with an anodic peak current of 15.5 μA . It is possible to observe the increase in magnification of the anodic peak current for the ND/GCE at $1.3\times$ compared to the bare electrode. This difference is due to the larger electroactive surface area of the ND/GCE, which enables a greater number of electronic reactions on the surface of the electrode.

Also, the electron transfer rate between the electroactive material and the surface of the electrode greatly increased after the modification with ND, resulting in an increase in the oxidation peak current of PAR on the ND/GCE and a negative shift in the peak potential. Notably, after the modification with ND, the electroactive surface area increased by $2.6\times$, and electrocatalytic activity favored the occurrence of PAR oxidation reactions at more negative potentials compared to the unmodified electrode. This difference might be attributed to the oxidation of PAR, a diffusion-controlled process that occurs in an irreversible reaction on the electrode surface [43–45].

According to Mahmoud et al., PAR oxidation involves a process of 2 e^- and 2 H^+ transfer to form a quinone-like structure, followed by hydrolysis of the acetamide functional group to produce p-aminophenol, a process demonstrated in Figure 4B [46]. SWV voltammograms were recorded using the ND/GCE for both a blank solution and a $5.2 \mu\text{mol L}^{-1}$ PAR solution in 0.1 mol L^{-1} of H_2SO_4 to assess the electrode's performance.

The SWV technique was selected as the electroanalytical tool to perform the voltametric determination of PAR using the ND/GCE in this work. Thus, the parameters of this technique were all optimized to obtain a better analytical response with a high current magnitude and a well-defined voltametric profile. These parameters were evaluated in the following ranges: a frequency (f) of 10.0 to 100 Hz, an amplitude (a) of 5.00 to 100 mV, and a step potential (s) of 1.0 to 10 mV. In this context, the optimum values were $f = 80 \text{ Hz}$, $a = 40 \text{ mV}$, and $s = 6 \text{ mV}$.

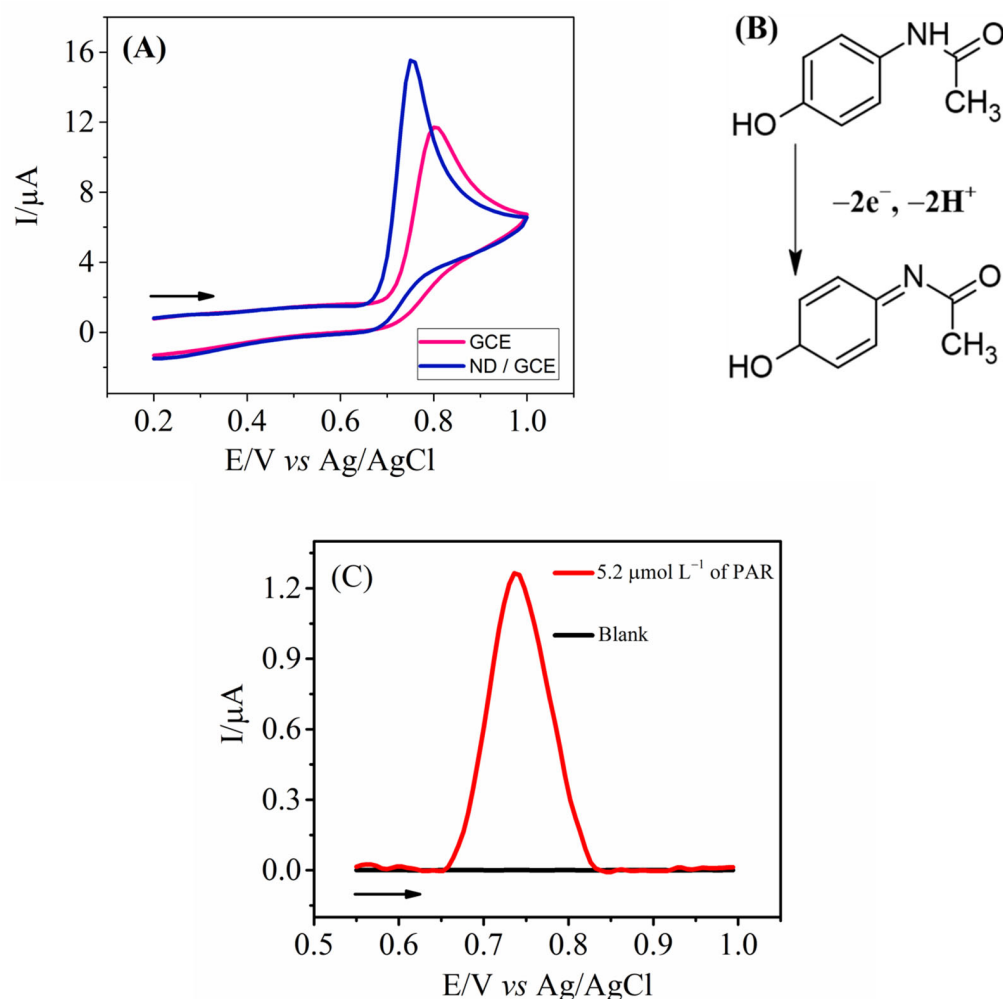


Figure 4. (A) Cyclic voltammograms obtained in the presence of $5.0 \times 10^{-3} \text{ mol L}^{-1}$ PAR in $0.1 \text{ mol L}^{-1} \text{ H}_2\text{SO}_4$ at a scan rate of 50 mV s^{-1} ; (B) the suggested mechanism for PAR oxidation on ND/GCE; (C) SWV voltammograms were obtained for blank solution and $5.2 \mu\text{mol L}^{-1}$ of PAR in $0.1 \text{ mol L}^{-1} \text{ H}_2\text{SO}_4$ solution using the ND/GCE; analysis condition: $f = 25 \text{ Hz}$, $a = 20 \text{ mV}$ and $\Delta E_s = 5 \text{ mV}$.

Under the optimum conditions, the analytical curve for PAR was constructed using the modified electrochemical sensor. Figure 5A shows the voltammograms obtained in the presence of different PAR concentrations, and the analytical curve presented in Figure 5B shows a linear response in the concentration range of 0.79 to $100 \mu\text{mol L}^{-1}$ ($0.79, 2.31, 3.78, 5.2, 8.86, 12.5, 19.7, 26.7, 33.6, 69.1, 86.7,$ and $100 \mu\text{mol L}^{-1}$) for PAR with a linear correlation coefficient of 0.998 , following equation $I (\mu\text{A}) = 0.1344 C_{\text{PAR}} (\mu\text{mol L}^{-1}) + 1.24 \times 10^{-7}$.

This linearity represents that this system works mostly through the diffusion process. The LOD was equal to $0.18 \mu\text{mol L}^{-1}$, calculated by $3 \times \text{RSD blank/slope}$.

To evaluate the repeatability and reproducibility of the proposed method, the ND/GCE was subjected to this study. The concentration of PAR to perform these studies was $5.2 \mu\text{mol L}^{-1}$. Five measurements ($n = 5$) were obtained for the freshly prepared modified electrode, for repeatability, as shown in Figure S1A,B. Then, for reproducibility, the determination of paracetamol was performed at a newly constructed modified electrode on five different days ($n = 5$), as shown in Figure S1C,D. The relative standard deviation (RSD) of repeatability and reproducibility was calculated to be 1.8% and 5.1% , respectively, demonstrating the method's satisfactory results.

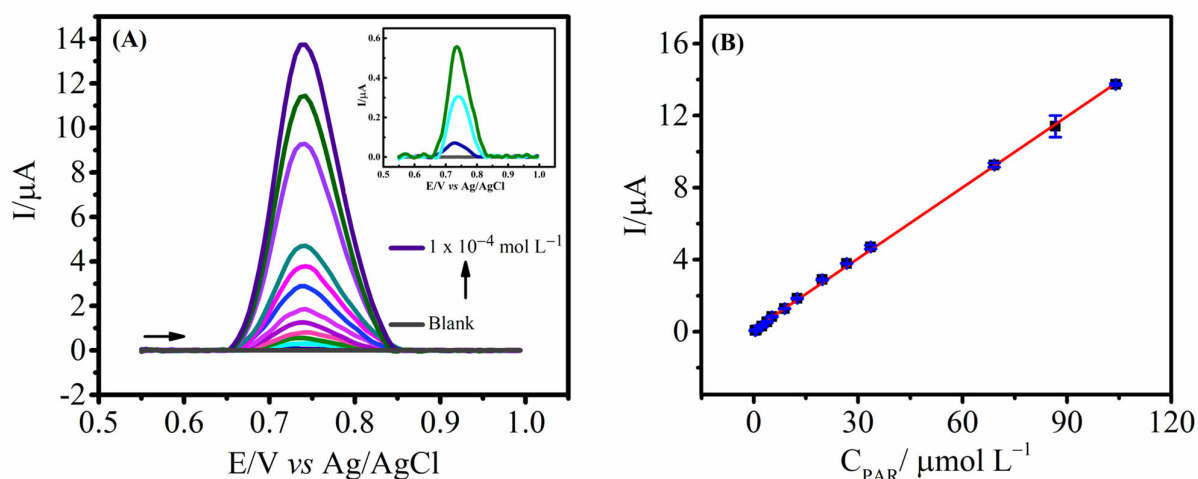


Figure 5. (A) SWV records were obtained for different PAR concentrations: (1) 0.0 (blank solution), and (2 to 13) 0.79, 2.31, 3.78, 5.2, 8.86, 12.5, 19.7, 26.7, 33.6, 69.1, 86.7, and 100 $\mu\text{mol L}^{-1}$ in 0.1 mol L^{-1} of H_2SO_4 solution using the ND/GCE. Analysis condition: $f = 80$ Hz, $a = 40$ mV, and $\Delta E_s = 6$ mV. Inset: PAR concentrations in 0.0 (blank), 0.79, 2.31, and 3.78 $\mu\text{mol L}^{-1}$. (B) Analytical curve (I_p versus C_{PAR}).

To evaluate the practical utility and validity of the ND/GCE, the modified electrode was applied to the detection of the analyte in commercial tablets with two different concentrations of PAR, 500 and 750 mg/tablet. The samples were performed in three replicate measurements for each concentration. The determination of paracetamol with the same electrode surface at every measurement produced a mean recovery of 96.4 and 98.7%. From the results obtained, the ND/GCE demonstrated good electrocatalytic activity. Good recovery indicates the suitability and reliability of the proposed method. Therefore, the ND/GCE is reliable and recommended for routine analyses of PAR in pharmaceutical samples.

The application of the ND/GCE in pharmaceutical samples (prepared as described in the experimental section) analysis was investigated via spectrophotometry and voltammetry. The electrochemical results were obtained using SWV records with the proposed method, to which aliquots of a stock solution were consecutively added to the electrochemical cell. The peak currents showed a direct relationship with the PAR concentration present in pharmaceutical samples. Table 1 presents the results obtained using the proposed and comparative spectrophotometric method in the pharmaceutical samples. Furthermore, a comparison of the results obtained for pharmaceutical samples using the proposed and comparative methods resulted in RSDs ranging from 1.4 and 1.8%. From the results, it is possible to observe the accuracy of both methods, with a low percentage of error, which reinforces the satisfactory analytical response for the ND/GCE sensor and its successful application for the determination of the analyte in these types of samples. A selectivity evaluation for this electrode toward PAR was indeed conducted. Tests were performed with several potential concomitant species, including cysteine (CYS), sodium chloride (NaCl), potassium chloride (KCl), ascorbic acid (AA), dopamine (DA), and glucose (GLU); see Figure S2. The interference solutions were prepared using equal concentrations of the interferent and PAR in a 0.1 mol L^{-1} H_2SO_4 solution. None of the tested species exceeded 10.47% of interference; see Table S2. Moreover, no additional peaks were observed in any of the measurements for these analytes; see Figure S3.

Table 1. Results obtained in the determination of PAR in pharmaceutical samples.

| Samples | PAR (mg/Tablet) | | |
|---------|---------------------------------|------------------------------|---------------------------------|
| | Comparative Method ^a | Proposed Method ^a | Relative Error ^b (%) |
| A | 496 ± 3 | 503 ± 2 | 1.4 |
| B | 739 ± 8 | 752 ± 4 | 1.8 |

^a Average of three measured concentrations. ^b Relative error = ((proposed method—comparative method)/comparative method) × 100%.

Several studies can be found in the literature in which the surface of a GCE was modified to determine paracetamol, as demonstrated in Table 2. Among them, Mehretie et al. [47] determined the analyte with the modification of PEDOT (poly(3,4-ethylene dioxythiophene)); they obtained a linear range of 1.0 to 100 $\mu\text{mol L}^{-1}$ and an LOD = 4.0 mol L^{-1} , being applied to samples of pharmaceutical products and biological fluids. Awad et al. [48] obtained a sensor with a linear detection range for PAR from 3.0×10^{-3} to 6.5×10^{-3} mol L^{-1} with an LOD of 2.8×10^{-4} mol L^{-1} using an electrochemically activated glassy carbon electrode. In the work of Li et al. [49], a PAR sensor was developed with a GCE modified using PANI-MWCNTs (polyaniline and multiwalled carbon nanotubes), with a linear range of 1.0×10^{-6} to 2.0×10^{-4} mol L^{-1} and an LOD = 2.5×10^{-7} mol L^{-1} . Kassem et al. [50] also studied the determination of PAR through an electrochemically activated glassy carbon electrode using copper nanoparticles, which resulted in a sensor with a linear range of 4.0×10^{-6} to 2.8×10^{-5} mol L^{-1} and an LOD equal to 3.5×10^{-7} mol L^{-1} . Finally, Kang et al. [45] performed a GCE modification with graphene for PAR sensing, with a linear range of 1.0×10^{-7} to 2.0×10^{-5} mol L^{-1} and an LOD = 3.2×10^{-8} mol L^{-1} . Thereby, the proposed sensor showed a wide linear range for the detection of PAR, with a low LOD in comparison to other sensors. When compared to other works, the proposed method of PAR determination is characterized by satisfactory sensitivity, significantly higher than for sensors based on copper nanoparticles or multi-walled carbon nanotubes. However, it is smaller in comparison to the LOD for the graphene/GCE sensor, and even with that, it presents as analytically acceptable for the analyte. Additionally, the proposed sensor does not require a long time for the construction and application of composite materials or enzymatic and molecular imprinting technologies. Thus, the proposed sensor architecture is characterized by a simple and highly reproducible procedure, being an excellent candidate for PAR determination.

Table 2. Analytical characteristics of electroanalytical methods reported for PAR determination.

| Electrode | Technique | Linear Range (mol L^{-1}) | LOD (mol L^{-1}) | Reference |
|------------------|-----------|--|-----------------------------|-----------|
| PEDOT/GCE | DPV | 2.5×10^{-6} to 2.0×10^{-4} | 1.1×10^{-6} | [47] |
| GCoX/GCE | LSV | 3.0×10^{-3} to 6.5×10^{-3} | 2.8×10^{-3} | [48] |
| PANI-MWCNT/GCE | SWV | 1.0×10^{-6} to 2.0×10^{-4} | 2.5×10^{-7} | [49] |
| nano-Cu/GCoX/GCE | SWV | 4.0×10^{-6} to 2.8×10^{-5} | 3.5×10^{-7} | [50] |
| Graphene/GCE | SWV | 1.0×10^{-7} to 2.0×10^{-5} | 3.2×10^{-8} | [45] |
| ND/GCE | SWV | 7.9×10^{-7} to 1.0×10^{-4} | 1.8×10^{-7} | This work |

Abbreviations: PEDOT: poly(3,4-ethylene dioxythiophene); GCE: glassy carbon electrode; carbon ionic liquid electrode; GCoX: electro-activated glassy carbon electrode; PANI: polyaniline; MWCNT: multi-walled carbon nanotubes; nano-Cu: copper nanoparticles.

4. Conclusions

Surface modification with nanomaterials can provide an advantage in sensor sensitivity. The present work has demonstrated the successful application of an ND/GCE electrode as an electrochemical sensor for the determination of PAR in pharmaceutical samples. Cyclic voltammetry and square-wave voltammetry were used for the characterization of electrochemical behavior, the optimization of experimental and instrumental parameters, and PAR determination. When applied to pharmacological samples, the pro-

posed sensor was shown to be a simple, fast, and inexpensive method compared to other analytical methods usually used for drug determination, showing a good analytical response to detecting and quantifying PAR. Thereby, the ND/GCE sensor presents a wide linear range for the determination of PAR from 7.9×10^{-7} to 1.0×10^{-4} mol L⁻¹, with an LOD = 1.8×10^{-7} mol L⁻¹ and analytical sensitivity equal to 1.3×10^{-6} μA mol L⁻¹. The analytical utility of the method was successfully demonstrated in the analysis of PAR tablet samples, which obtained rates of recovery of 96.4 and 98.7%. Furthermore, the electrochemical device presents stability and satisfactory repeatability.

Supplementary Materials: The following supporting information can be downloaded at <https://www.mdpi.com/article/10.3390/chemosensors12110243/s1>. Figure S1: Repeatability and reproducibility of ND/GCE. (A) SWV records were obtained for five measurements in a row using 5.2 μmol L⁻¹ of PAR in 0.1 mol L⁻¹ H₂SO₄ solution; (B) Current vs Scans in the same system; (C) SWV records were obtained for five different modifications using 5.2 μmol L⁻¹ of PAR in 0.1 mol L⁻¹ H₂SO₄ solution; (D); Current vs days in the different systems; Table S1: Calculated values of electroactive area and heterogeneous electron transfer rate constant (k₀) for GCE and ND/GCE; Table S2: Percentage of Interference from Potential Concomitant Species; Figure S2: Results obtained (%) for interference study using different species for PAR determination. Supporting electrolyte: 0.1 mol L⁻¹ H₂SO₄; Figure S3. SWV records were obtained for different concomitant species using equal concentrations of the interferents: Cysteine (CYS), Sodium Chloride (NaCl), Potassium Chloride (KCl), Ascorbic Acid (AA), Dopamine (DA) and Glucose (GLU) and PAR in 0.1 mol L⁻¹ H₂SO₄ solution. Analysis condition: f = 80 Hz, a = 40 mV and ΔEs = 6 mV.

Author Contributions: Conceptualization: D.d.O.L., F.M.M., P.B.D., A.N., J.R.C., R.C.d.F., L.V.B., O.F.F., B.C.J. and G.G.d.O.; methodology: D.d.O.L., F.M.M., P.B.D., A.N., J.R.C., R.C.d.F., L.V.B., O.F.F., B.C.J. and G.G.d.O.; validation: D.d.O.L., F.M.M., P.B.D., A.N., J.R.C., R.C.d.F., L.V.B., O.F.F., B.C.J. and G.G.d.O.; formal analysis: D.d.O.L., F.M.M., P.B.D., A.N., J.R.C., R.C.d.F., L.V.B., O.F.F., B.C.J. and G.G.d.O.; investigation, D.d.O.L., F.M.M., P.B.D., A.N., J.R.C., R.C.d.F., L.V.B., O.F.F., B.C.J. and G.G.d.O.; resources: D.d.O.L., F.M.M., P.B.D., A.N., J.R.C., R.C.d.F., L.V.B., O.F.F., B.C.J. and G.G.d.O.; data curation: D.d.O.L., F.M.M., P.B.D., A.N., J.R.C., R.C.d.F., L.V.B., O.F.F., B.C.J. and G.G.d.O.; writing—original draft preparation: D.d.O.L., F.M.M., P.B.D., A.N., J.R.C., R.C.d.F., L.V.B., O.F.F., B.C.J. and G.G.d.O.; writing—review and editing: D.d.O.L., F.M.M., P.B.D., A.N., J.R.C., R.C.d.F., L.V.B., O.F.F., B.C.J. and G.G.d.O.; supervision: B.C.J. and G.G.d.O.; project administration: B.C.J. and G.G.d.O.; funding acquisition: B.C.J. and G.G.d.O. All authors have read and agreed to the published version of the manuscript.

Funding: The authors are grateful for the financial support provided by the following Brazilian agencies: the São Paulo State Research Support Foundation (FAPESP, #2019/00166-2, #2024/03497-8, #2023/06793-4 and #2023/02963-2), Tocantins State Research Support Foundation (FAPT), the Brazilian National Council for Scientific and Technological Development (CNPq #401681/2023-8 and #406079/2022-6(nanovida) INCT NanoAgro #405924/2022-4, #308439/2021-0, #145563/2024-3, and #381660/2024-9), and Coordenação de Aperfeiçoamento de Pessoal de Nível Superior—Brasil (#88887.986513/2024-00 and MEC-CAPES INCTNanoAgro #88887.953443/2024-00).

Institutional Review Board Statement: Not applicable.

Informed Consent Statement: Not applicable.

Data Availability Statement: Data is contained within the article or Supplementary Materials.

Acknowledgments: The authors are grateful for the financial support provided by the following Brazilian agencies: the São Paulo State Research Support Foundation (FAPESP, #2019/00166-2, #2024/03497-8, #2023/06793-4 and #2023/02963-2), Tocantins State Research Support Foundation (FAPT), the Brazilian National Council for Scientific and Technological Development (CNPq #401681/2023-8 and #406079/2022-6(nanovida) INCT NanoAgro #405924/2022-4, #308439/2021-0, #145563/2024-3, and #381660/2024-9), and Coordenação de Aperfeiçoamento de Pessoal de Nível Superior—Brasil (#88887.986513/2024-00 and MEC-CAPES INCTNanoAgro #88887.953443/2024-00).

Conflicts of Interest: The authors declare no conflicts of interest.

References

1. Mochalin, V.N.; Shenderova, O.; Ho, D.; Gogotsi, Y. The properties and applications of nanodiamonds. *Nat. Nanotechnol.* **2012**, *7*, 11–23. [[CrossRef](#)] [[PubMed](#)]
2. Kulakova, I.I. Surface chemistry of nanodiamonds. *Phys. Solid State* **2004**, *46*, 636–643. [[CrossRef](#)]
3. Silva, L.R.G.; Carvalho, J.H.S.; Stefano, J.S.; Oliveira, G.G.; Prakash, J.; Janegitz, B.C. Electrochemical sensors and biosensors based on nanodiamonds: A review. *Mater. Today Commun.* **2023**, *35*, 106142. [[CrossRef](#)]
4. Petrov, I.L.; Shenderova, O.A. History of Russian patents on detonation nanodiamonds. In *Ultrananocrystalline Diamond*; Elsevier: Amsterdam, The Netherlands, 2006; pp. 559–588.
5. Chauhan, S.; Jain, N.; Nagaich, U. Nanodiamonds with powerful ability for drug delivery and biomedical applications: Recent updates on in vivo study and patents. *J. Pharm. Anal.* **2020**, *10*, 1–12. [[CrossRef](#)]
6. Prabhakar, N.; Rosenholm, J.M. Nanodiamonds for advanced optical bioimaging and beyond. *Curr. Opin. Colloid Interface Sci.* **2019**, *39*, 220–231. [[CrossRef](#)]
7. Gu, W.; Peters, N.; Yushin, G. Functionalized carbon onions, detonation nanodiamond and mesoporous carbon as cathodes in Li-ion electrochemical energy storage devices. *Carbon* **2013**, *53*, 292–301. [[CrossRef](#)]
8. Basso, L.; Cazzanelli, M.; Orlandi, M.; Miotello, A. Nanodiamonds: Synthesis and Application in Sensing, Catalysis, and the Possible Connection with Some Processes Occurring in Space. *Appl. Sci.* **2020**, *10*, 4094. [[CrossRef](#)]
9. Qin, J.-X.; Yang, X.-G.; Lv, C.-F.; Li, Y.-Z.; Chen, X.-X.; Zhang, Z.-F.; Zang, J.-H.; Yang, X.; Liu, K.-K.; Dong, L.; et al. Humidity Sensors Realized via Negative Photoconductivity Effect in Nanodiamonds. *J. Phys. Chem. Lett.* **2021**, *12*, 4079–4084. [[CrossRef](#)] [[PubMed](#)]
10. Wong, A.; Materón, E.M.; Freitas, T.A.; Faria, R.C.; Gonçalves, D.; Del Pilar Taboada Sotomayor, M. Voltammetric sensing of tryptophan in dark chocolate bars, skimmed milk and urine samples in the presence of dopamine and caffeine. *J. Appl. Electrochem.* **2022**, *52*, 1249–1257. [[CrossRef](#)]
11. Camargo, J.R.; Baccarin, M.; Raymundo-Pereira, P.A.; Campos, A.M.; Oliveira, G.G.; Fatibello-Filho, O.; Oliveira, O.N.; Janegitz, B.C. Electrochemical biosensor made with tyrosinase immobilized in a matrix of nanodiamonds and potato starch for detecting phenolic compounds. *Anal. Chim. Acta* **2018**, *1034*, 137–143. [[CrossRef](#)]
12. Dai, W.; Li, M.; Gao, S.; Li, H.; Li, C.; Xu, S.; Wu, X.; Yang, B. Fabrication of Nickel/nanodiamond/boron-doped diamond electrode for non-enzymatic glucose biosensor. *Electrochim. Acta* **2016**, *187*, 413–421. [[CrossRef](#)]
13. Simioni, N.B.; Oliveira, G.G.; Vicentini, F.C.; Lanza, M.R.V.; Janegitz, B.C.; Fatibello-Filho, O. Nanodiamonds stabilized in dihexadecyl phosphate film for electrochemical study and quantification of codeine in biological and pharmaceutical samples. *Diam. Relat. Mater.* **2017**, *74*, 191–196. [[CrossRef](#)]
14. Simioni, N.B.; Silva, T.A.; Oliveira, G.G.; Fatibello, O. A nanodiamond-based electrochemical sensor for the determination of pyrazinamide antibiotic. *Sens. Actuators B-Chem.* **2017**, *250*, 315–323. [[CrossRef](#)]
15. Qin, J.-X.; Yang, X.-G.; Lv, C.-F.; Li, Y.-Z.; Liu, K.-K.; Zang, J.-H.; Yang, X.; Dong, L.; Shan, C.-X. Nanodiamonds: Synthesis, properties, and applications in nanomedicine. *Mater. Des.* **2021**, *210*, 110091. [[CrossRef](#)]
16. Shirani, A.; Hu, Q.; Su, Y.; Joy, T.; Zhu, D.; Berman, D. Combined Tribological and Bactericidal Effect of Nanodiamonds as a Potential Lubricant for Artificial Joints. *ACS Appl. Mater. Interfaces* **2019**, *11*, 43500–43508. [[CrossRef](#)]
17. Miller, B.S.; Bezing, L.; Gliddon, H.D.; Huang, D.; Dold, G.; Gray, E.R.; Heaney, J.; Dobson, P.J.; Nastouli, E.; Morton, J.J.L.; et al. Spin-enhanced nanodiamond biosensing for ultrasensitive diagnostics. *Nature* **2020**, *587*, 588–593. [[CrossRef](#)] [[PubMed](#)]
18. Jozwiak-Bebenista, M.; Nowak, J.Z. Paracetamol: Mechanism of Action, Applications and Safety Concern. *Acta Pol. Pharm.* **2014**, *71*, 11–23.
19. de Martino, M.; Chiarugi, A. Recent Advances in Pediatric Use of Oral Paracetamol in Fever and Pain Management. *Pain Ther.* **2015**, *4*, 149–168. [[CrossRef](#)] [[PubMed](#)]
20. Du, K.; Ramachandran, A.; Jaeschke, H. Oxidative stress during acetaminophen hepatotoxicity: Sources, pathophysiological role and therapeutic potential. *Redox Biol.* **2016**, *10*, 148–156. [[CrossRef](#)]
21. Jaeschke, H.; McGill, M.R.; Williams, C.D.; Ramachandran, A. Current issues with acetaminophen hepatotoxicity-A clinically relevant model to test the efficacy of natural products. *Life Sci.* **2011**, *88*, 737–745. [[CrossRef](#)]
22. Olaleye, M.T.; Rocha, B.T.J. Acetaminophen-induced liver damage in mice: Effects of some medicinal plants on the oxidative defense system. *Exp. Toxicol. Pathol.* **2008**, *59*, 319–327. [[CrossRef](#)] [[PubMed](#)]
23. Fernandez, C.; Heger, Z.; Kizek, R.; Ramakrishnappa, T.; Borun, A.; Faisal, N.H. Pharmaceutical Electrochemistry: The Electrochemical Oxidation of Paracetamol and Its Voltammetric Sensing in Biological Samples Based on Screen Printed Graphene Electrodes. *Int. J. Electrochem. Sci.* **2015**, *10*, 7440–7452. [[CrossRef](#)]
24. Mazer, M.; Perrone, J. Acetaminophen-induced nephrotoxicity: Pathophysiology, clinical manifestations. *J. Med. Toxicol.* **2008**, *4*, 2–6. [[CrossRef](#)]
25. Knochen, M.; Giglio, J.; Reis, B.F. Flow-injection spectrophotometric determination of paracetamol in tablets and oral solutions. *J. Pharm. Biomed. Anal.* **2003**, *33*, 191–197. [[CrossRef](#)] [[PubMed](#)]
26. Srivastava, M.K.; Ahmad, S.; Singh, D.; Shukla, I.C. Titrimetric Determination of Dipyrone and Paracetamol with Potassium Hexacyanoferrate(III) in an Acidic Medium. *Analyst* **1985**, *110*, 735–737. [[CrossRef](#)]

27. dos Santos, W.T.P.; Gimenes, D.T.; de Almeida, E.G.N.; Eiras, S.D.; Albuquerque, Y.D.T.; Richter, E.M. Simple Flow Injection Amperometric System for Simultaneous Determination of Dipyrone and Paracetamol in Pharmaceutical Formulations. *J. Braz. Chem. Soc.* **2009**, *20*, 1249–1255. [[CrossRef](#)]
28. Felix, F.S.; Brett, C.M.A.; Angnes, L. Carbon film resistor electrode for amperometric determination of acetaminophen in pharmaceutical formulations. *J. Pharm. Biomed. Anal.* **2007**, *43*, 1622–1627. [[CrossRef](#)]
29. Vaughan, P.A.; Scott, L.D.L.; McAleer, J.F. Amperometric Biosensor for the Rapid-Determination of Acetaminophen in Whole-Blood. *Anal. Chim. Acta* **1991**, *248*, 361–365. [[CrossRef](#)]
30. Xu, Z.M.; Yue, Q.; Zhuang, Z.J.; Xiao, D. Flow injection amperometric determination of acetaminophen at a gold nanoparticle modified carbon paste electrode. *Microchim. Acta* **2009**, *164*, 387–393. [[CrossRef](#)]
31. Sayed, M.; Ismail, M.; Khan, S.; Khan, H.M. A comparative study for the quantitative determination of paracetamol in tablets using UV-Visible spectrophotometry and high performance liquid chromatography. *Phys. Chem.* **2015**, *17*, 1–5.
32. Narwade, S.S. Qualitative and Quantitative Analysis of Paracetamol in Different Drug Samples by HPLC Technique. *IOSR J. Appl. Chem.* **2014**, *7*, 46–49. [[CrossRef](#)]
33. Biswas, S.; Chakraborty, D.; Das, R.; Bandyopadhyay, R.; Pramanik, P. A simple synthesis of nitrogen doped porous graphitic carbon: Electrochemical determination of paracetamol in presence of ascorbic acid and p-aminophenol. *Anal. Chim. Acta* **2015**, *890*, 98–107. [[CrossRef](#)] [[PubMed](#)]
34. Kannan, A.; Sevel, R. A highly selective and simultaneous determination of paracetamol and dopamine using poly-4-amino-6-hydroxy-2-mercaptopyrimidine (Poly-AHMP) film modified glassy carbon electrode. *J. Electroanal. Chem.* **2017**, *791*, 8–16. [[CrossRef](#)]
35. Anvisa. Insumos farmacêuticos e especialidades: Monografias. *Farm. Bras.* **2019**, *II*, 904.
36. Baccarin, M.; Rowley-Neale, S.J.; Cavalheiro, É.; Smith, G.C.; Banks, C.E. Nanodiamond based surface modified screen-printed electrodes for the simultaneous voltammetric determination of dopamine and uric acid. *Microchim. Acta* **2019**, *186*, 200. [[CrossRef](#)]
37. Bouali, W.; Kurtay, G.; Genç, A.A.; Ahmed, H.E.H.; Soylak, M.; Erk, N.; Karimi-Maleh, H. Nanodiamond (ND)-Based ND@CuAl₂O₄@Fe₃O₄ electrochemical sensor for Tofacitinib detection: A unified approach to integrate experimental data with DFT and molecular docking. *Environ. Res.* **2023**, *238*, 117166. [[CrossRef](#)]
38. da Silva, V.A.O.P.; Tartare, V.A.P.; Kalinke, C.; Oliveira, P.R.d.; Souza, D.C.d.; Bonacin, J.A.; Janegitz, B.C. Lab-made 3D-printed contact angle measurement adjustable holder. *Química Nova* **2020**, *43*, 1312–1319.
39. Pacheco, W.F.; Semaan, F.S.; Almeida, V.G.K.; Ritta, A.G.S.L.; Aucélio, R.Q. Voltammetry: A Brief Review About Concepts. *Rev. Virtual Química* **2013**, *5*, 516–537. [[CrossRef](#)]
40. Ferreira, N.G.; Silva, L.L.G.; Corat, E.J.; Trava-Airoldi, V.J. Kinetics study of diamond electrodes at different levels of boron doping as quasi-reversible systems. *Diam. Relat. Mater.* **2002**, *11*, 1523–1531. [[CrossRef](#)]
41. Nicholson, R.S. Theory and application of cyclic voltammetry for measurement of electrode reaction kinetics. *Anal. Chem.* **1965**, *37*, 1351–1355. [[CrossRef](#)]
42. Lavagnini, I.; Antiochia, R.; Magno, F. An Extended Method for the Practical Evaluation of the Standard Rate Constant from Cyclic Voltammetric Data. *Electroanal. Int. J. Devoted Fundam. Pract. Asp. Electroanal.* **2004**, *16*, 505–506. [[CrossRef](#)]
43. Sanghavi, B.J.; Srivastava, A.K. Simultaneous voltammetric determination of acetaminophen, aspirin and caffeine using an in situ surfactant-modified multiwalled carbon nanotube paste electrode. *Electrochim. Acta* **2010**, *55*, 8638–8648. [[CrossRef](#)]
44. ShangGuan, X.D.; Zhang, H.F.; Zheng, J.B. Electrochemical behavior and differential pulse voltammetric determination of paracetamol at a carbon ionic liquid electrode. *Anal. Bioanal. Chem.* **2008**, *391*, 1049–1055. [[CrossRef](#)] [[PubMed](#)]
45. Kang, X.; Wang, J.; Wu, H.; Liu, J.; Aksay, I.A.; Lin, Y. A graphene-based electrochemical sensor for sensitive detection of paracetamol. *Talanta* **2010**, *81*, 754–759. [[CrossRef](#)] [[PubMed](#)]
46. Mahmoud, B.G.; Khairy, M.; Rashwan, F.A.; Banks, C.E. Simultaneous Voltammetric Determination of Acetaminophen and Isoniazid (Hepatotoxicity-Related Drugs) Utilizing Bismuth Oxide Nanorod Modified Screen-Printed Electrochemical Sensing Platforms. *Anal. Chem.* **2017**, *89*, 2170–2178. [[CrossRef](#)]
47. Mehretie, S.; Admassie, S.; Hunde, T.; Tessema, M.; Solomon, T. Simultaneous determination of N-acetyl-p-aminophenol and p-aminophenol with poly(3,4-ethylenedioxythiophene) modified glassy carbon electrode. *Talanta* **2011**, *85*, 1376–1382. [[CrossRef](#)]
48. Awad, M.I.; Sayqal, A.; Pashameah, R.A.; Hameed, A.M.; Morad, M.; Alessa, H.; Shah, R.K.; Kassem, M.A. Enhanced Paracetamol Oxidation and Its Determination using Electrochemically Activated Glassy Carbon Electrode. *Int. J. Electrochem. Sci.* **2021**, *16*, 150864. [[CrossRef](#)]
49. Li, M.Q.; Jing, L.H. Electrochemical behavior of acetaminophen and its detection on the PANI-MWCNTs composite modified electrode. *Electrochim. Acta* **2007**, *52*, 3250–3257. [[CrossRef](#)]
50. Kassem, M.A.; Awad, M.I.; Morad, M.; Aljandali, B.A.; Pashameah, R.A.; Alessa, H.; Mohammed, G.I.; Sayqal, A. Sensor based on Copper Nanoparticles Modified Electrochemically Activated Glassy Carbon Electrode for Paracetamol Determination. *Int. J. Electrochem. Sci.* **2022**, *17*, 2. [[CrossRef](#)]

Disclaimer/Publisher's Note: The statements, opinions and data contained in all publications are solely those of the individual author(s) and contributor(s) and not of MDPI and/or the editor(s). MDPI and/or the editor(s) disclaim responsibility for any injury to people or property resulting from any ideas, methods, instructions or products referred to in the content.